Environmental Research 197 (2021) 111140



Contents lists available at ScienceDirect

Environmental Research

journal homepage: www.elsevier.com/locate/envres





Green synthesis of bio-functionalized nano-particles for the application of copper removal – characterization and modeling studies

A. Muthu Kumara Pandian [a,*], B. Gopalakrishnan [b], M. Rajasimman [b], N. Rajamohan [c], C. Karthikeyan [b]

[a] Department of Biotechnology, Vivekanandha College of Engineering for Women, Tiruchengode, Namakkal, 637205, India
[b] Environmental Engineering Laboratory, Department of Chemical Engineering, Annamalai University, Annamalai Naga, 608002, Tamilnadu, India
[c] Chemical Engineering Section, Faculty of Engineering, Sohar University, Oman

ARTICLE INFO

Keywords:
Copper
Ag nanoparticles
Halimeda gracilis
Sorption
RSM

ABSTRACT

Green technology for the synthesis of nanoparticles has gained momentum due to its cost-effectiveness and eco-friendly nature. In this research study, silver nanoparticles (AgNps) were synthesized using an eco-friendly biological method involving the use of marine algae, *Halimeda gracilis*. The surface properties of the synthesized silver nanoparticles were studied using UV–visible spectroscopy, Fourier transform infrared spectroscopy and scanning electron microscopy methods. During the synthesis of nano particles, the parameters namely temperature (30 °C to 90 °C), pH (6–10), silver nitrate ($AgNO_3$) concentration (1–3 mg/ml) and quantity of algal extract (1–3 ml) were optimized to improve the production of AgNPs. The application of the synthesized silver nanoparticles for the adsorptive removal of copper from aqueous and industrial wastewater was investigated. Intra-particle diffusion mechanism was identified to be controlling step in metal removal. Regeneration of sorbent was carried out using 2.0 M HCl and the reusability was verified for 6 cycles. A removal efficiency of copper (64.8%) from electroplating wastewater demonstrated the industrial application potential of the synthesized silver nanoparticles.

1. Introduction

Nanomaterials have gained significant importance for application in environmental, biomedical, energy, biotechnology and related fields of engineering and science due to its high activity, specificity and effectiveness. Nanomaterials are tailor-made in terms of the end-user requirement and equipped with performance-oriented properties like high surface area, high electrical conductivity, enhanced thermal and optical characteristics (Yaqoob et al., 2020). Nanomaterials are found to be used in three principal forms namely nanoparticle, nanofiber and nanoplate (Chauhan et al., 2019). The global applications of nanomaterials have involved more than 1800 products with an estimated capital investment of 150 billion US$ in USA only. Silver nanoparticle, identified as a potential contributor in various applications, has been reported to reach 800 tonnes production capacity globally, by 2025 (Calderon-Jimenez et al., 2017). Nanoparticles are synthesized using multiple routes namely physical, chemical, photochemical and biological methods. Each of these techniques has its own merits and de-merits (Marimuthu et al., 2020). Due to comparatively higher use of chemicals, high temperature requirement and cost, physico-chemical techniques are less preferred. Biological methods are favored in terms of eco-friendliness and sustainability.

Silver nanoparticles present a class of nanomaterials which has found extensive use for potential applications in environmental pollution control. Moreover, the effectiveness of the nanoparticle in the specific application is determined by its structure formation and molecule orientation. The choice of silver nanoparticles for use as a sorbent is related to the favorable properties like very high surface area per unit volume, higher affinity to specific target ions and environmental friendliness. Several biological methods, using plant, fungi or bacteria mediation, for silver nanoparticles synthesis are found to be efficient in terms of characteristics of the nanomaterial produced (Muthukumarapandian et al., 2021).

Copper, one of the most widely metals in industrial activities, has been identified as a toxic contaminant released into waste waters emanating from metallurgical plants, electrochemical industries, battery

* Corresponding author.
E-mail address: dr.mkpandian@gmail.com (A. Muthu Kumara Pandian).

https://doi.org/10.1016/j.envres.2021.111140
Received 11 February 2021; Received in revised form 1 April 2021; Accepted 4 April 2021
Available online 14 April 2021
0013-9351/© 2021 Elsevier Inc. All rights reserved.

Table 1
BBD and its Response for *H.gracilis* mediated AgNp production.

Run No.	A	B	C	D	Quantity of AgNp, g	
					Experimental	Predicted
1	1	−1	0	0	0.7	0.879
2	0	0	0	0	2.0	2.033
3	1	0	0	−1	2.4	2.408
4	0	0	−1	1	2.1	2.096
5	1	0	0	1	2.5	2.542
6	−1	−1	0	0	0.5	0.463
7	0	0	1	1	2.2	2.246
8	0	1	0	1	2.5	2.579
9	1	1	0	0	2.7	2.746
10	0	0	1	0	1.7	1.746
11	1	0	0	0	2.1	2.033
12	0	0	1	0	2.7	2.563
13	0	1	1	−1	1.8	1.812
14	−1	−1	0	−1	0.8	0.629
15	0	1	0	0	2.2	2.029
16	−1	0	−1	−1	2.1	2.062
17	−1	0	0	1	2.0	2.075
18	0	0	0	−1	1.7	1.742
19	−1	1	−1	0	2.4	2.375
20	0	0	−1	0	2.0	2.046
21	0	0	0	0	2.0	2.033
22	1	0	−1	0	2.5	2.362
23	0	−1	0	1	0.7	0.463
24	0	−1	1	0	0.5	0.608
25	0	−1	−1	0	0.3	0.458
26	0	1	0	−1	1.8	1.946
27	0	1	1	0	2.2	2.125

Table 2
ANOVA for *H.gracilis* mediated synthesis of AgNp.

Source	Sum of Squares	Df	Mean Square	F-value	P-value
Model	13.50	14	0.96	40.96	<0.0001
A	0.96	1	0.96	40.92	<0.0001
B	8.84	1	8.84	375.54	<0.0001
C	7.500	1	7.500	0.32	0.5829
D	0.16	1	0.16	6.94	0.0218
AB	0.023	1	0.023	0.96	0.3476
AC	0.063	1	0.063	2.65	0.1292
AD	1.000	1	1.000	0.42	0.5268
BC	0.040	1	0.040	1.70	0.2169
BD	0.16	1	0.16	6.80	0.0229
CD	0.040	1	0.040	1.70	0.2169
A^2	0.11	1	0.11	4.55	0.0543
B^2	2.22	1	2.22	94.49	<0.0001
C^2	9.259	1	9.259	3.933	0.9510
D^2	1.481	1	1.481	0.063	0.8062
Residual	0.28	12	0.024		
Lack of fit	0.28	10	0.028	8.27	0.1126
Pure error	6.667	2	3.333		
Cor total	13.78	26			

making industries and mining activities (Harsha Vardhan et al., 2019). The presence of copper in the released water poses a huge threat to the natural ecosystem due to its non-biodegradable nature and easy entry into the food chain through aquatic organisms. Copper is reported to get accumulated in soil and other exposed environmental component. The permissible concentration of copper, according to United States Environmental Protection Agency, is reported as 2 ppm (Al-Saydeh et al., 2017). Excess consumption of copper can lead to kidney failure, liver damage and reduced functioning of nervous system (Fernandez-Gonzalez et al., 2020). Regulations imposed by the pollution control authorities demand the treatment of copper polluted water before discharged into natural streams. The methods available for the removal of copper includes physico-chemical techniques like adsorption, coagulation, ion exchange, cementation, dialysis, electrodialysis and membrane processes (Rajamohan and Rajasimman, 2016). Even though these methods have specific advantages related to removal efficiency, they

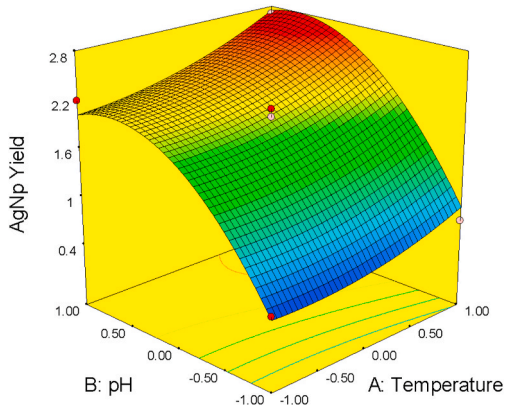


Fig. 1. Effect of pH & temperature on *H.gracilis* mediated AgNp Production.

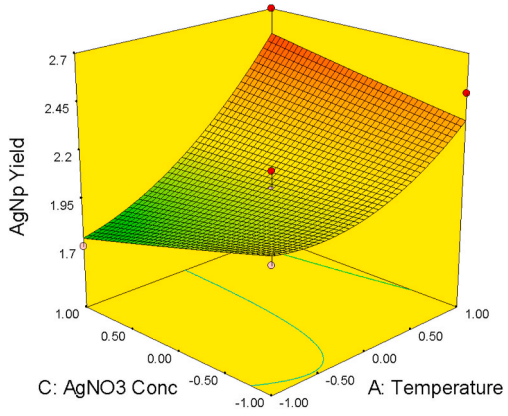


Fig. 2. Effect of concentration of $AgNO_3$ & temperature on *H.gracilis* mediated AgNp production.

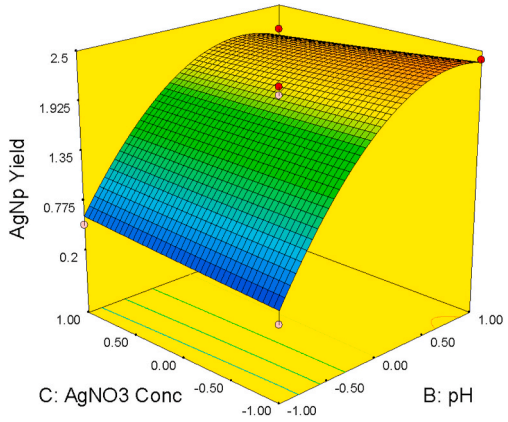


Fig. 3. Effect of concentration of $AgNO_3$ & pH on *H.gracilis* mediated AgNp production.

suffer from disadvantages like reduced effectiveness at lower metal concentration, presence of co-pollutant, higher operating costs and secondary pollution. Studies on removal of copper using modified wheat straw (Dong et al., 2019), honeycomb-like porous activated carbon (Mondal et al., 2019), microbiologically modified carbonate precipitation (Duarte-Nass et al., 2020), algal biomass (Gunasundari and Senthilkumar, 2017), Azadirachta indica seeds (Davi Costa et al., 2020) and hydrolyzed olive cake (Fernandez-Gonzalez et al., 2020).

Optimization tools, aimed at identifying the best operating conditions for any waste water treatment, are helpful in the design of

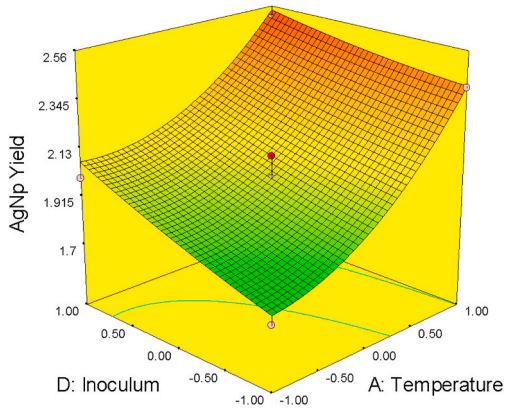


Fig. 4. Effect of quantity of extract & temperature on *H.gracilis* mediated AgNp production.

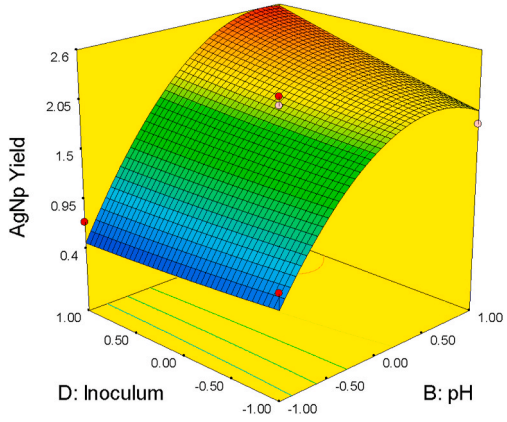


Fig. 5. Effect of quantity of extract & pH on *H.gracilis* mediated AgNp production.

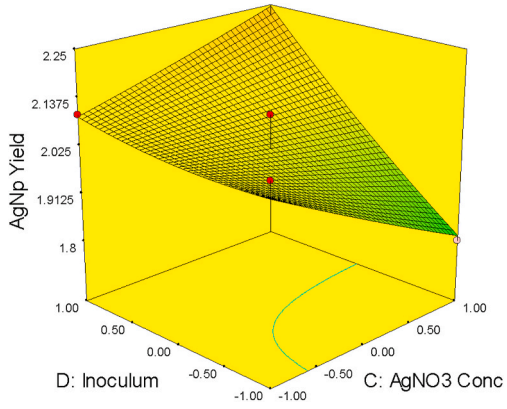


Fig. 6. Effect of quantity of extract & concentration of $AgNO_3$ on *H.gracilis* mediated AgNp *p*roduction.

experiments. Response Surface Methodology based experiments are well documented and employed approaches using central composite design, Box Benken design (Jayakumar et al., 2015; Venkatesh babu et al., 2017; Rajasimman et al., 2021). No detailed studies are reported for the application of algae based nanoparticle for the removal of copper. Biologically mediated nanoparticle is identified as a potential choice for the removal of copper. This research work involves investigation on the synthesis and characterization of marine algae, *Halimedia Gracilis*, facilitated synthesis of silver nanoparticles and application for the removal of copper. The effect of operating variables, namely temperature, pH, concentration of $AgNO_3$ and quantity of extract, on the formation of silver nanoparticles, was studied. Using Box Benken Design (BBD), the optimization of parameters to screen the most influencing variables was investigated. The characterization of the silver nanoparticles was carried out using SEM and Fourier Transform Infra-Red (FTIR) spectroscopy.

2. Materials and methods

Stock solution of desired concentration was prepared using Copper sulphate, $CuSO_4$ (Merck Ltd, India). Silver nitrate and the buffer components, NaOH and HCl, were purchased (Himedia labs, India). The stock solution containing copper of 1000 ppm was prepared by dissolving 3.801 g of Cu (SO_4) in 1000 ml of de-ionized water. The working solution was prepared from the stock solution, by diluting it to appropriate volumes. The pH of the working solutions was adjusted with HCl or NaOH.

2.1. Silver nanoparticle preparation

The synthesis of nano particle was investigated using the algal biomass, *Halimeda gracilis* The algae was collected, size-reduced and ground to fine powder. A predetermined mass, 6 g of powdered *Halimeda gracilis* was taken and added to 50 ml of de-ionized water and the resultant mixture is kept at room temperature. The solids were removed from the solution after 24 h. The extract was taken and 50 ml of 10^{-3} M Silver nitrate was added. After completion of 120 min, the appearance of light orange color change was noted and the presence of silver nanoparticles was confirmed. This solution was allowed for 48 h to give a dark brown color. The extract was filtered using Whatman filter paper (No.42) to remove the large aggregates. The extract was then lyophilized to get the silver nanoparticles.

2.2. Maximization of silver nanoparticle production

Silver nano particle synthesis was dependent on the choice of optimal conditions. The operating variables chosen for study includes temperature, pH, concentration of silver nitrate and quantity of extract and the experiments were performed using Box–Behnken design. The influence of temperature on the yield of nanoparticles using *H.gracilis* was studied by varying the temperature from 30 °C to 90 °C. The influence of pH on the nanoparticle production using *H.gracilis* was carried out by varying the pH from 6 to 10. The pH of the working solution was adjusted with HCl or NaOH. Silver nitrate was used as precursor of silver nanoparticle production by all methods. The effect of silver nitrate concentration on silver nanoparticle production was carried out in the range of 1–3 mg/ml. The effect of quantity of extract on silver nanoparticle production was carried out by varying the algae extract from 1 to 3 ml.

2.3. Batch sorption experiment

During the batch experiments, 100 ml of the sorbate - sorbent mixture was taken in 250 ml Erlenmeyer flask and incubated in a laboratory shaker (Thomas Scientific, USA). The samples were centrifuged in the high speed centrifuge at 10,000 rpm (Drucker, USA) and the supernatant concentrations were analyzed using atomic absorption spectrophotometer (Shimadzu, Japan). After making triplicate measurements, the obtained results were statistically analyzed. The pollutant uptake per unit mass of silver nanoparticles (q_e, mg/g) is obtained using the following expression:

$$q_e = \frac{(C_o - C_e)V}{m} \quad (1)$$

The quantity of adsorbed metal/unit mass of adsorbent at time t (q_t

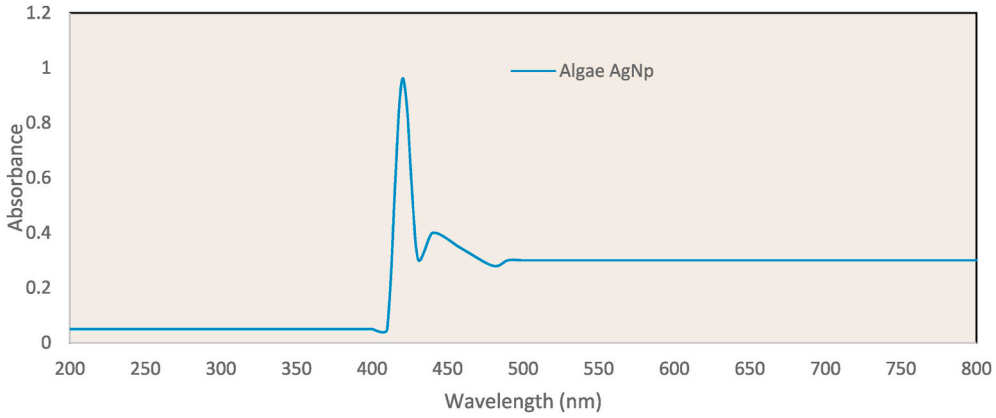


Fig. 7. UV–Visible spectra for *H.gracilis* mediated AgNp.

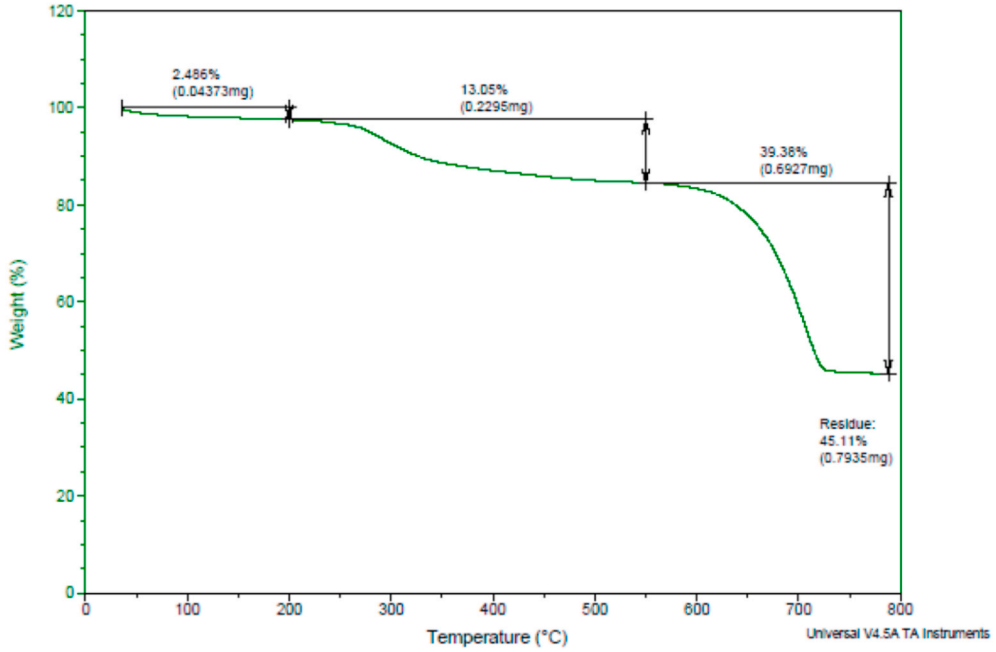


Fig. 8. TGA curve for synthesized AgNP particle.

Table 3
BBD and copper removal results using *H.gracilis* mediated AgNp.

Run no	A	B	C	% Cu (II) removal	
				Experimental	Predicted
1	0	1	−1	69.00	69.50
2	0	1	1	76.00	76.50
3	0	−1	1	39.00	38.50
4	−1	0	1	85.00	83.50
5	1	−1	0	30.00	31.00
6	1	1	0	71.00	69.00
7	0	0	0	77.00	77.00
8	1	0	1	74.00	73.50
9	0	0	0	76.00	77.00
10	0	0	0	78.00	77.00
11	0	−1	−1	35.00	32.50
12	−1	1	0	78.00	77.00
13	1	0	−1	67.00	68.50
14	−1	0	−1	75.00	75.50
15	−1	−1	0	38.00	40.00

Table 4
ANOVA for removal of copper using *H.gracilis* mediated AgNp.

Source	Sum of Squares	df	Mean Square	F-value	P-value
Model	4815.60	9	535.07	89.18	<0.0001
A	144.50	1	144.50	24.08	0.0044
B	2812.50	1	2812.50	468.75	<0.0001
C	84.50	1	84.50	14.08	0.0133
AB	0.25	1	0.25	0.042	0.8463
AC	2.25	1	2.25	0.37	0.5671
BC	0.25	1	0.25	0.042	0.8463
A^2	2.83	1	2.83	0.47	0.5230
B^2	1766.83	1	1766.83	294.47	<0.0001
C^2	2.83	1	2.83	0.47	0.5230
Residual	30.00	5	6.00		
Lack of fit	28.00	3	9.33	9.33	0.0983
Pure error	2.00	2	1.00		
Cor total	4845.60	14			

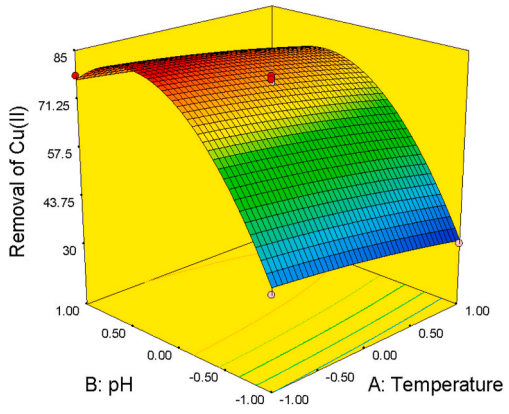


Fig. 9. Effect of pH and temperature on sorption of copper using *H.gracilis* mediated AgNp.

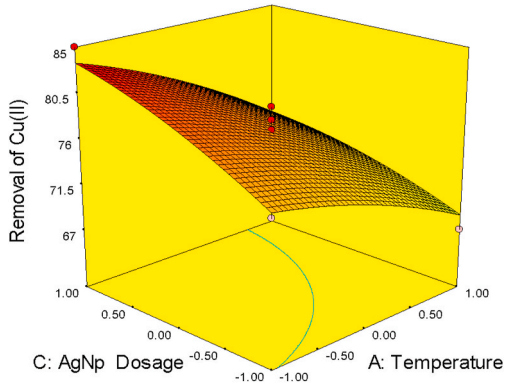


Fig. 10. Effect of temperature and AgNp dosage on sorption of copper using *H. gracilis* mediated AgNp.

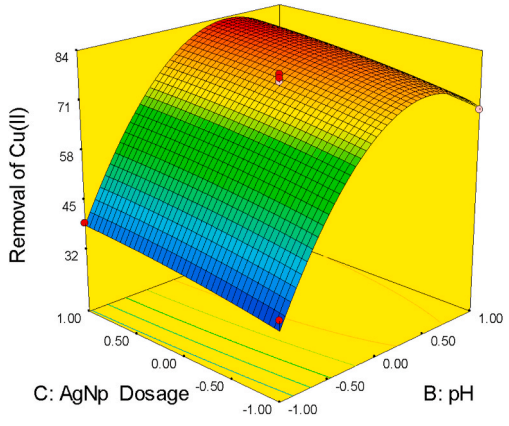


Fig. 11. Effect of pH and AgNp dosage on sorption of copper using *H.gracilis* mediated AgNp.

mg/g) is obtained using the following expression:

$$q_t = \frac{(C_o - C_t)V}{m} \tag{2}$$

where V - Volume of solution treated (L), C_o – Initial metal concentration (mg/L), C_e - Equilibrium concentration of metal (mg/L), C_t - Concentration of adsorbents at time t (mg/L), m - Sorbent mass (g). In the first set of experiments, the variation on the sorption of copper onto the synthesized nanoparticle was investigated in the pH range of 5–9. The effect of operating temperature on the metal removal performance of the nanoparticle was studied in the range of 30 °C to 60 °C. The quantity of the nanoparticle was varied from 0.1 to 0.9 g, by simultaneously varying the conditions of pH and temperature. All the experiments were performed in triplicates and the average values were reported.

2.4. Characterization of silver nanoparticles

The characteristics of the synthesized silver nanoparticles were analyzed in the range 200–800 nm, using UV–visible scanning. The presence of silver was confirmed by Lambda max. The double beam analysis of the sample was done using water as the blank. The reduction of silver nitrate (Ag^+ ions) to silver nanoparticles (Ag^0) was monitored by analyzing the samples using double beam spectrophotometer (Systronics, India). SEM imaging of the silver nanoparticles before and after treatment were recorded. (JEOL, Japan) with an accelerating voltage of 20 KV, at high vacuum (HV) mode. Thermogravimetric analysis (TGA) was carried out to study the thermal stability of the synthesized nanoparticles using TGA (SDT Q600, TA Instruments, USA).

The functional group identification of the synthesized nanoparticles was carried out using FTIR spectrophotometer (Thermo Scientific –Nicolet iS_5 FTIR, USA) in the spectral range, 4000–400 cm^{-1}. During the analysis, 1:10 mass ratio was used with the sample and KBr pellets.

3. Results and discussion

3.1. Halimeda gracilis mediated AgNp production

The statistical optimization tool, namely BBD design, was implemented for the synthesis of algae mediated silver nano particles. The theoretical and experimental values of the quantity of nanoparticles produced were given in Table 1.

The quantity of AgNP produced was predicted by:

$$\begin{aligned}\text{AgNp, g} &= 2.03 + 0.28A + 0.86B - 0.025C + 0.12D + 0.075AB \\ &+ 0.12AC - 0.050AD - 0.1BC + 0.20BD + 0.1CD + 0.14A^2 - 0.65B^2 \\ &- 4.167C^2 + 0.017D^2\end{aligned} \tag{3}$$

where A - temperature, B – pH, C - concentration of $AgNO_3$, D – quantity of algae extract.

The ANOVA for Ag Np synthesis were tabulated in Table 2. The fitness of model was confirmed by F value (40.96) and R^2 (0.9795). A low deviation between experimental and predicted values was also confirmed by a low CV value (8.44).

Std. Dev.- 0.15; R-Squared- 0.9795; Mean - 1.82; Adj R-Squared- 0.9556; C.V. %- 8.44; Pred R-Squared- 0.8836; PRESS- 1.60; Adeq Precision- 20.002.

Adeq precision value of 20.002 indicates a good signal. In this work, A, B, D, B^2 and BD were significant model terms for the maximum production of nanoparticles.

Temperature was varied in the range of 30–90 °C and its effect on the quantity of silver nanoparticles produced was presented in Figs. 1, 2 and 4. With increase in temperature, the yield of nano particles increased and thus confirmed the endothermic nature of the process. Similar results on production of silver nanoparticles were reported with maximum production attained at 90 °C (Ravichandran et al., 2011). The presence of hydrogen ions, measured in terms of pH, was reported to influence the ionic strength of the medium in which silver nanoparticles were produced. As shown in Figs. 1, 3 and 5, the pH effect was investigated over the range 5.0–9.0 and maximum yield of nanoparticles was obtained at pH 8.6. Reduced productivity of silver nanoparticles in the acidic pH range were reported in related studies (Vanaja et al., 2014; Bankar et al., 2010). Availability of favorable functional groups at basic pH was found to be the reason for the increased synthesis. In addition, inactivation of

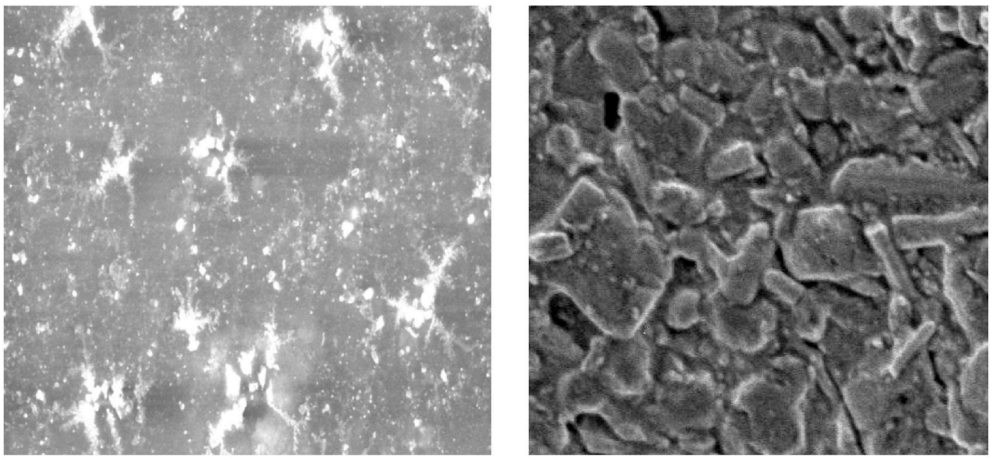


Fig. 12. (a) AgNp before sorption Fig. 11(b) AgNp after sorption.

algal surface at acidic pH was reported to influence the synthesis of silver nanoparticles (Sathishkumar et al., 2009).

The concentration of the base compound (Silver nitrate) is reported to influence the extent of formation of silver nanoparticles. In this set of experiments, the concentration of silver nitrate was varied in the range of 1–3 mg/ml and the quantity of silver nanoparticles produced were recorded. From Figs. 2, 3 and 6, the optimal quantity of silver nitrate yielding maximum production of the silver nanoparticles was identified as 3 mg/ml. Efficient conversion of the substrate compound by the algal components was reported to occur in specific proportions (Rastogi and Arunachalam, 2013).

The volume of extract, a key operating variable, was varied in the range of 1–3 ml and the variations in the quantity of silver nanoparticles synthesized were observed. A directly proportional relationship was found to exist between the volume of extract and the quantity of silver nano particles synthesized. The requirement of higher extract volumes was confirmed by Figs. 4–6. From the different parametric experiments, the conditions favoring maximum production of 2.72 g/100 ml of *Halimeda gracilis* mediated silver nanoparticles were identified as: pH-8.6, temperature - 90 °C, concentration of $AgNO_3$ – 3 mg/ml and volume of extract - 3 ml.

3.2. UV–visible spectroscopy analysis and TGA analysis

The formation reaction of silver nanoparticles was verified by visual changes in color and the appearance of dark brown after the completion was noticed. Surface plasmon resonance was reported to be the mechanism of this change (Mie 1908). The characterization studies conducted have confirmed the presence of AgNps in the wavelength range, 350 nm–450 nm (Kadir et al., 2005). As shown in Fig. 7, the peak absorption at 420 nm confirmed the presence of AgNps. The TGA curve for the synthesized silver nano particles in the temperature range of 30–800 °C, was shown in Fig. 8. The AgNP shows excellent thermal stability at low temperature. This observation was proved by relatively lesser weight loss (2.486%) up to 200 °C. In the temperature range, 200–550 °C, the loss in weight was found as 13.05% and a sharp decline in weight was observed above 550°. Through this study, thermal stability of the synthesized silver nanoparticle was found to be much better.

3.3. Sorption of copper (II) using Halimeda gracilis mediated AgNp

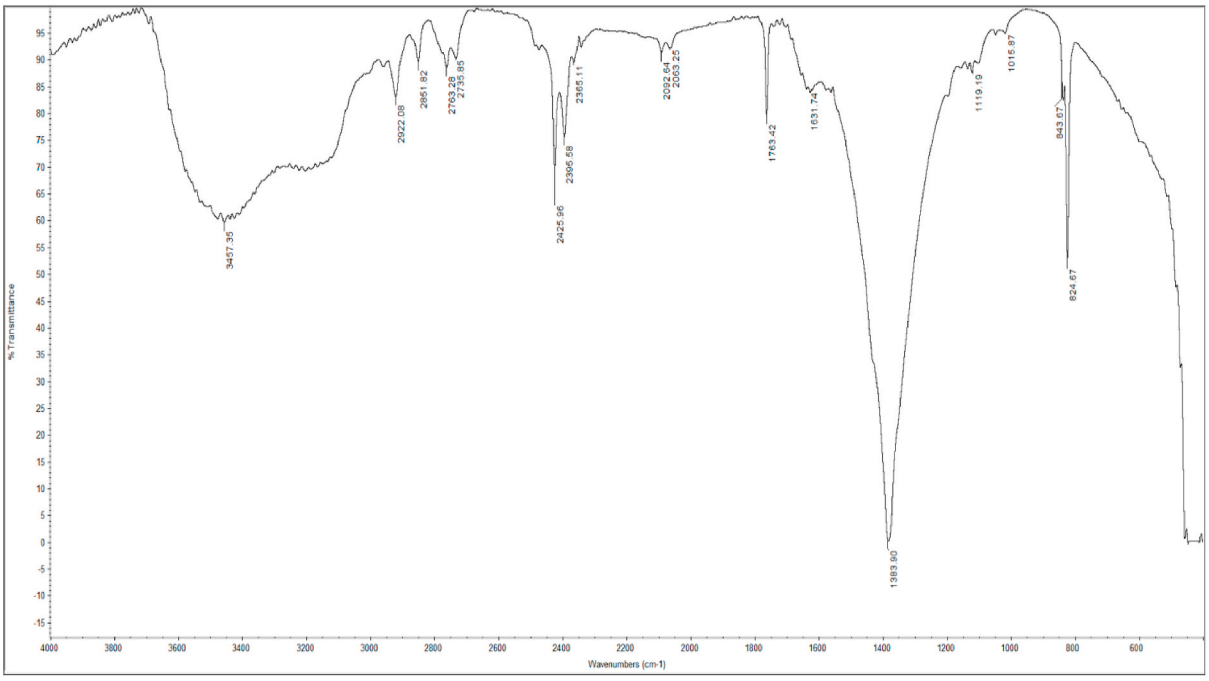
The sorption results of copper using the synthesized nanoparticles was performed based on the BBD (Table 3). The removal of copper was predicted using:

$$Copper\ \ removal, \% = 77.00 - 4.25A + 18.75B + 3.25C + 0.25AB - 0.00AC + 0.25BC - 0.87A^2 - 21.87B^2 - 0.87C^2 \quad (4)$$

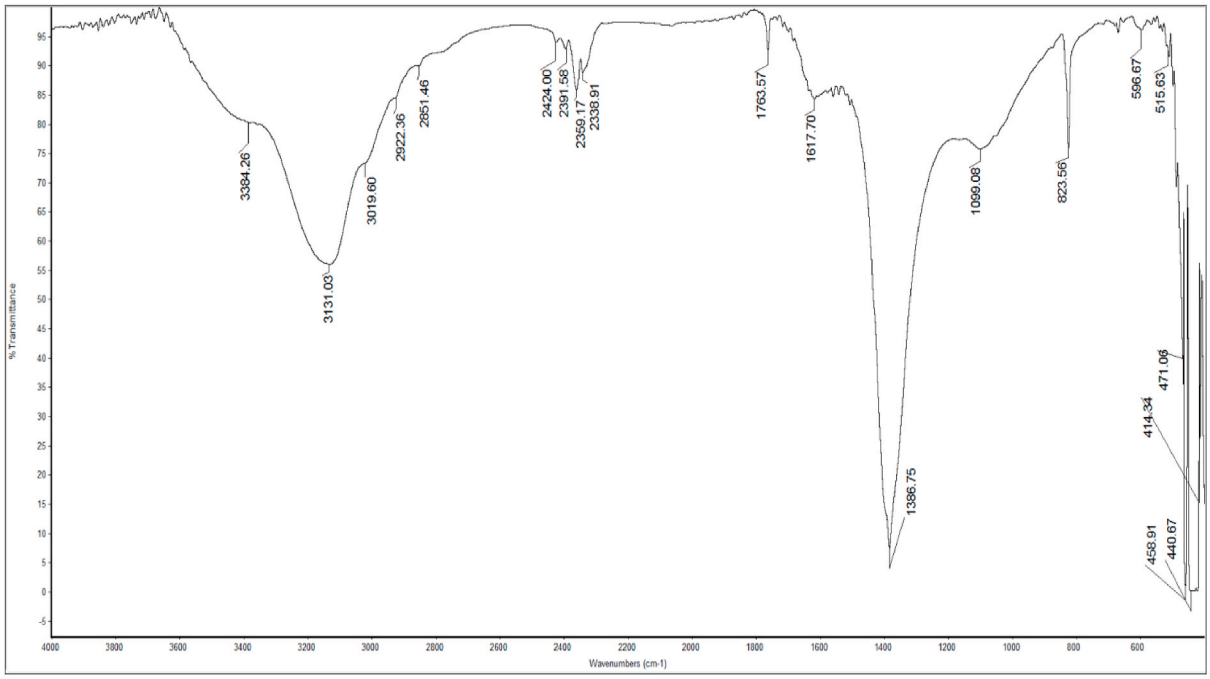
where A – pH; B – temperature; and C - nanoparticles dosage. Table 4 presents the data on statistical variance estimates. The value of the parameters (F = 89.18 and R^2 = 0.9938) confirmed the suitability of the model. The experimental and predicted data were compared and there was no significant variations as confirmed by low value of CV. The significant model parameters identified through this study were A, B, C and B^2.

The influence of metal solution pH on the removal performance of the synthesized silver nanoparticles was studied and the results were presented in Figs. 9 and 11. The optimal pH range suitable for better removal efficiencies was found to be 7.5–9.0. The pH which produced maximum copper removal by silver nanoparticles was found to be 7.8. The recued metal removal patterns observed at acidic pH values were related to the enhanced repulsion of copper cations by the hydrogen ions and occupancy of the surface-active sites by the hydrogen ions as competitive ions (Rajeshkannan et al., 2010). Temperature variations can play a major role in altering the adsorption rate due to its influence on solubility. As shown in Figs. 9 and 10, the optimal temperature for better sorption of copper onto the silver nanoparticle was found to be 30 °C. The negative impact of higher temperatures on the metal removal efficiency could be related to the alteration of surface characteristics and detachment of adsorbed metal ions (Volesky, 2003). The ratio between the surface sites and adsorbate ions is a key influencing variable and the quantity of nanoparticles added was varied from 0.1 to 0.9 g/100 ml to identify the optimal dose. As shown in Figs. 10 and 11, the effect of dosage was found to be dependent on interactive effect between pH and temperature. Better removal efficiencies achieved with increase in nanoparticle dosage was related to the higher ratio of active sites with the copper ions (Karimi et al., 2012). At pH 7.8 and temperature 30 °C, the maximum copper removal (85%) was found to be achieved at the optimal dose of 0.9 g/100 ml.

Std. Dev.- 2.45; R-Squared- 0.9938; Mean - 64.40; Adj R-Squared- 0.9827; C.V. %- 3.80; Pred R-Squared- 0.9066; PRESS- 452.50; Adeq Precision- 26.250.



(a) FTIR spectra of *H.gracilis* mediated AgNp before sorption



(b) FTIR spectra of *H.gracilis* mediated AgNp after sorption

Fig. 13. (a) FTIR spectra of *H.gracilis* mediated AgNp before sorption. Fig. 13 (b) FTIR spectra of *H.gracilis* mediated AgNp after sorption.

Table 5
FTIR analysis of AgNp before and after sorption of Cu (II).

Wavelength range (cm^{-1})	*H.gracilis* Mediated AgNp			Assignment
	Before Sorption	After Sorption	Differences	
3500–3000	3457.35	3384.26	−73.12	Bonded –OH groups
	–	3131.03	+3131.03	
	–	3019.60	+3019.60	
2900–2800	2922.08	2922.36	+0.32	CH stretching
	2851.82	2851.46	−0.36	
	2763.28	–	−2763.28	
	2735.85	–	−2735.85	
	2425.96	2424.00	−1.96	
	–	2391.58	+2391.58	
	2365.11	2359.17	−5.94	
	2092.64	–	+2092.64	
	2063.25	–	+2063.25	
1740–1680	1763.42	1763.57	+0.15	C=Ocarbonyl groups
	1631.74	1617.70	−14.04	
1500–1300	1383.90	1386.75	+2.85	C–O stretch
1150–850	1119.19	1099.08	−20.11	$-PO_4^{3-}$ stretching
	1015.37	–	−1015.37	
	843.67	–	−843.67	
	824.67	823.56	−1.11	
650–480	–	596.67	+596.67	N–containing bioligands
	–	515.63	+515.63	
	–	471.06	+471.06	
	–	458.91	+458.91	
	–	440.67	+440.67	
	–	414.34	+414.34	

Table 6
Isotherm model parameters for sorption of copper using synthesized AgNp.

Isotherm	Parameters	Value
	q_{max}, mg/g	46.2962
	B, l/mg	0.1821
	R^2	0.9709
Freundlich	K_f, l/mg	12.2574
	1/n	0.3279
	R^2	0.8121
D –R	q_{max}, mg/g	37.5848
	B, mol^2/kJ^2	1.1859
	E, kJ/mol	0.6568
	R^2	0.9031
Temkin	B, J/mol	8.3897
	K_T, l/mg	3.0789
	R^2	0.8133
Sips	a_s, l/mg	7.153
	K_s, l/mg	1.281
	β_s	0.1708
	R^2	0.8398

3.4. SEM analysis

The surface interaction between the silver nanoparticles and sorbate ion was investigated using the SEM imaging. As shown in Fig. 12 (a), existence of silver nanoparticles in isolation was observed before contacting the metal solution (size ranges from 100 to 2500 nm approx.). The effective interaction of sorbed metallic ions represented through the grouped existence was clearly evident in Fig. 12(b) The modification of the surface geometry before and adsorption proved that the occurrence of surface modifications.

3.5. FTIR analysis for Halimeda gracilis mediated AgNp

The functional groups responsible for the surface interaction of the synthesized silver nanoparticles with the sorbate ions were scanned using Fourier Transform Infra-Red spectroscopy. The spectrum, shown in Fig. 13 a, represents the surface characteristics before adsorption and key groups identified in the wavelength range of 3100–3400 cm^{-1} and 2800-2900 cm^{-1} corresponds to bonded –OH and stretching- CH groups, respectively (Table 5). The significant peak observed at 1631.74 cm^{-1} was attributed to the terpenoids related C═C stretching of aromatic ring The band at 2922.36 cm^{-1} shown in spectrum is assigned to the C–H stretching vibration of polymer backbone. The nanoparticle after adsorption of copper was analyzed and the spectrum was presented in Fig. 13(b). The appearance of new peaks and shifting of bands were observed and given in Table 5. Research study has reported that electrostatic and chemical adsorption were the causes of the shift in peaks observed (Dolphen and Thiravetyan, 2011). In addition, new peaks could be related to formation of new bonds due to change in molecular orientation as a result copper sorption (Ashish et al., 2017).

Table 7
Comparison of sorption capacities for removal of Cu (II).

Sorbent	Sorption capacity, mg/g	Source
Arthrobactor Species	40.44	Pagnanelli et al. (2001)
Cholerella vulgaris	76.71	Surya and Jai (2001)
Fucus vesiculosus	23.4	Grimm et al. (2008)
Enteromorpho prolifera	57.14	Ayla et al. (2009)
Scenedesmus quadricauda	75.6	Gulay and Yakup (2009)
Rocella phycopsis	37.8	Emine and Kadir (2010)
Cladophora Sp.	14.71	Yi and Shui (2011)
Spirogyra Sp.	38.61	Yi and Shui (2011)
Selenium nanoparticle	89	Yan Bai et al., 2011
SPIONs/PVA nano particle	47.594	Anudari Dolgormaa et al., 2018
SPIONs/gel/PVA nano particle	56.051	
Orange peel residue carbon nanoparticle	16.64	Elnaz Safari et al., 2019
Magnetic ferrite nanoparticles	124.80	Fang Liu et al., 2019
Fe3O4 nanoparticle	18.61	Jin Zhang et al., 2020
powdered activated carbon-magnetite nanoparticles composite	23.61	Meysam Shahrashoub and Somayeh Bakhtiari, 2021
Granular activated carbon-magnetite nanoparticles composite	13.37	
H.gracilis mediated AgNp	46.30	Present Study

Table 8
Kinetic model parameters for Cu (II) sorption using synthesized AgNp.

Kinetic Model	Parameters	Value
Pseudo first order	K_1 (min^{-1})	0.4769
	R^2	0.9629
Pseudo second order	K_2 ((g/mg)min)	0.0003
	R^2	0.7575
Intra particle diffusion	K_{id} ((mg/g)$min^{-0.5}$)	18.582
	R^2	0.9978
Power function	K	2.7150
	V	0.5317
	R^2	0.9894
Elovich	A(mg/g.min)	20.8539
	β	0.0671
	R^2	0.9722

3.6. Isotherm studies on sorption of Cu (II) using Halimeda gracilis, mediated AgNp

The equilibrium experiments conducted using various isotherms have been used to determine the maximum copper uptake capacity and tabulated in Table 6. Among the different isotherms tested, Langmuir isotherm provided the best fit and represented the possible presence of monolayer sorption with homogeneous. The equilibrium uptake (q_e) is estimated from the experimental data using Langmuir isotherm. The maximum uptake for Cu (II) is found to be 46.2962 mg/g, for *Halimeda gracilis*, mediated AgNp.

The sorption capacity attained in this study was compared with the other sorbents for the removal of Cu (II) and tabulated in Table 7. The

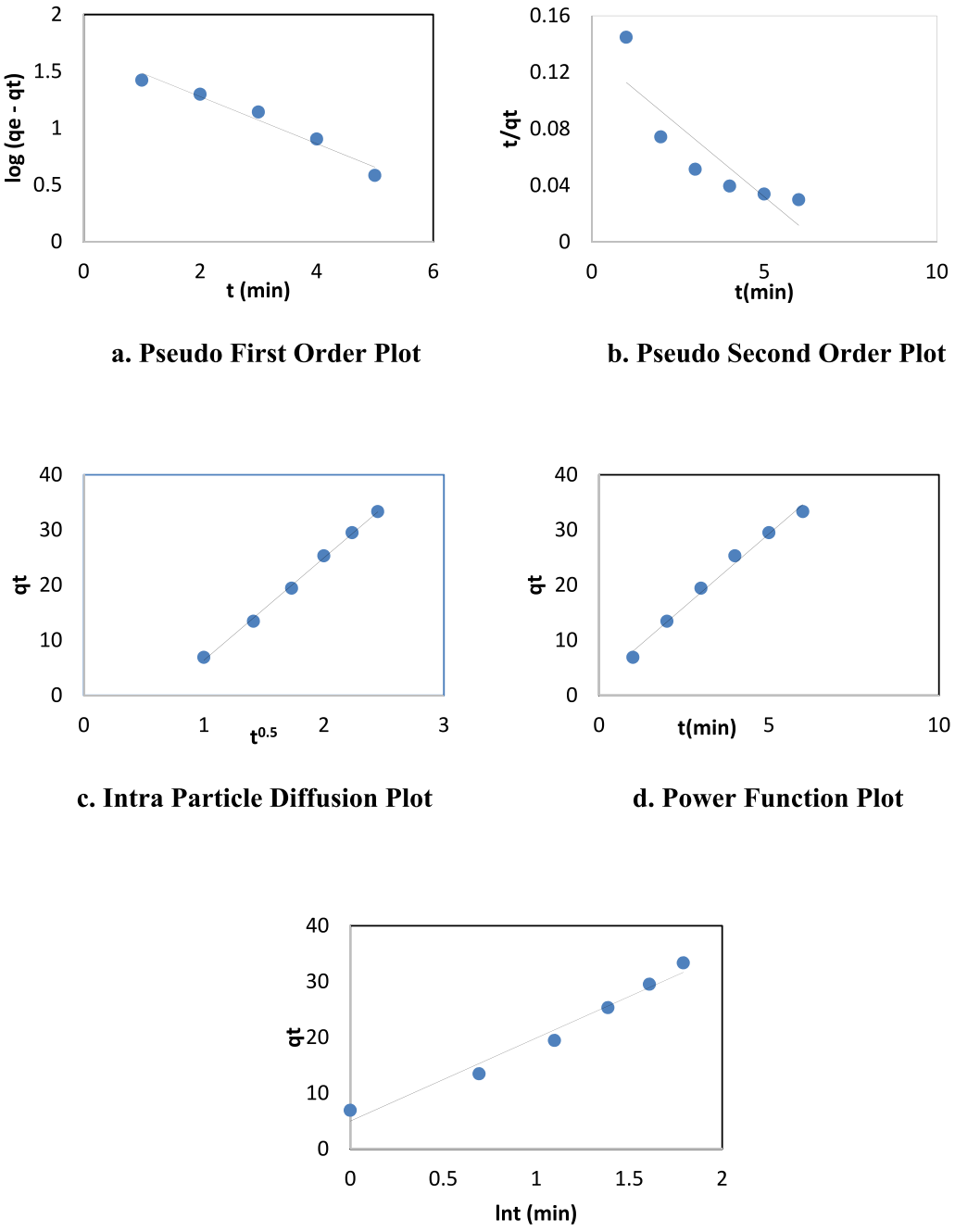


Fig. 14. Kinetic plot for sorption of Cu (II) using *Halimeda gracilis* mediated AgNp.

achievement of comparable copper uptake proved the suitability of the silver nanoparticles synthesized for efficient removal of Cu (II).

3.7. Sorption kinetics

The mechanism of metal sorption onto the silver nanoparticle was studied using the kinetic experiments. The three key steps identified to occur in any adsorption process are: diffusion in the bulk, diffusion into the surface pores and rapid uptake. The slowest step is assumed to be rate controlling mechanism (Ozer et al., 2006).

Pseudo I order model:

The pseudo first order equation (Ho, 2004) is represented by Eq (14):

$$\log(q_e - q_t) = \log q_e - \frac{K_1}{2.303} t \tag{14}$$

where q_t and q_e (mg/g) are the amounts of the dye adsorbed at equilibrium (mg/g) and t (min), respectively and K_1 is the rate constant of the equation (min^{-1}).

Pseudo II order model:

The pseudo second order model (Ho and McKay, 1999) is represented by Eq (15):

$$\frac{t}{q_t} = \frac{1}{K_2 q_e^2} + \frac{1}{q_e} t \tag{15}$$

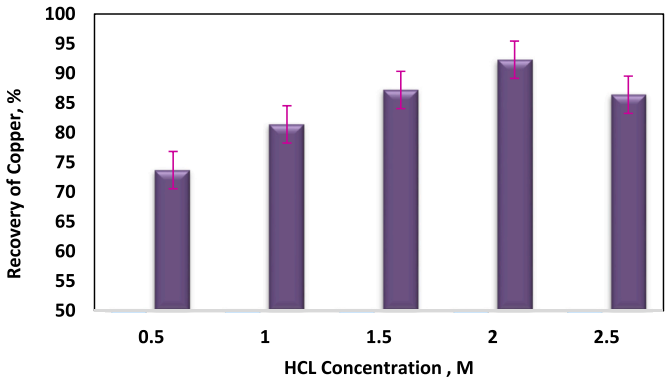


Fig. 15. Effect of Hcl concentration on desorption of Cu (II).

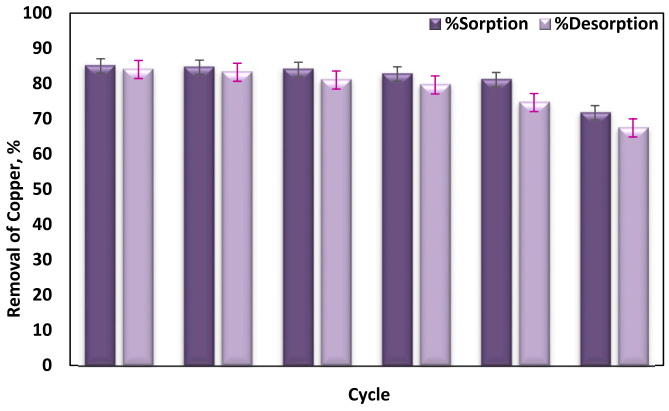


Fig. 16. Sorption – desorption cycles of Cu (II).

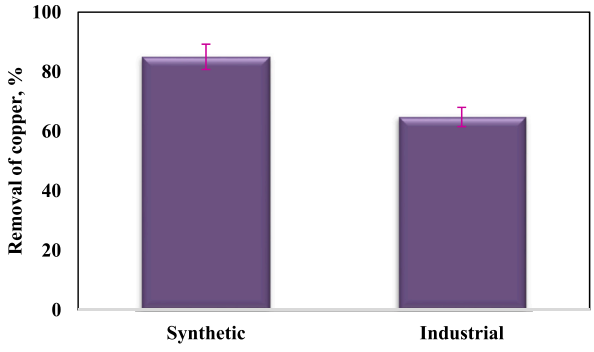


Fig. 17. Comparison of aqueous and electroplating industry wastewater.

where K_2 (g/mg min) – rate constant of the second-order equation, q_t (mg/g) – amount of sorption equilibrium (mg/g).

Intra particle diffusion model:

The model is given by Weber and Morris (1963) to relate the transport of the bulk liquid phase within the pores of the solid phase during the course of adsorption and is represented by Eq (16):

$$q_t = K_{id} t^{0.5} + C \tag{16}$$

where K_{id} - intraparticle diffusion rate constant (mg/g $min^{0.5}$) and C - intercept.

Power function model:

The power function (Aharoni et al., 1991) is represented by Eq (17):

$$q = K\, t^{v} \tag{17}$$

where q - amount of sorbate/unit mass of sorbent at time t, K and v are constants.

Elovich model:

The Elovich equation (Onal, 2006) which incorporates α - initial adsorption rate (mg/g min) and β (g/mg) - desorption constant, is represented by Eq (18):

$$q_t = \frac{1}{\beta} \ln \alpha\beta + \frac{1}{\beta} \ln(t) \tag{18}$$

where q_t - amount of gas sorbed at time t.

The experimental data were fitted with all the above said kinetic models. The estimated kinetic model parameters were given in Table 8. A higher value of R^2 for the intra particle diffusion model suggest the superiority of this model when compared with other kinetic models. From Fig. 14(a–e), the goodness of fit of the various models can be observed. The intraparticle diffusion rate constant, K_{id}, was estimated as 18.582.

3.8. Desorption and regeneration

The economic feasibility of the sorption process is ensured through the regeneration of sorbent and the ability of the adsorbent to retain its removal potential for multiple cycles. In this study, desorption of Cu (II) from the synthesized nanoparticles was studied by varying the HCl concentration from 0.5 M to 2.5 M and the outcomes were depicted in Fig. 15. The desorption of copper increased with increase in acid concentration up to 2 M of HCl and then decreased gradually.

The reuse of *Halimeda gracilis* was investigated by performing sorption experiments for six cycles. The copper sorbed onto the sorbents under investigation were eluted with 2.0 M HCl concentration. From the results depicted in Fig. 16, it was observed that the percentage of copper sorption remained consistently higher (>80%) from cycles 1 to 5 and decreased to 71.7% in the sixth cycle. This decrease in sorption might be a direct result of the algae lost during the sorption-desorption process. The reproducibility of the metal removal performance by the synthesized nanoparticles until five cycles proved the economic feasibility of this process.

3.9. Adsorption of Cu (II) from electroplating waste stream

Batch experiments were performed at the optimized conditions using electroplating waste stream. The results obtained from the sorption of copper from aqueous and electroplating effluent stream using the nanoparticle were shown in Fig. 17. Removal efficiency of copper was 85% for aqueous solution and 64.8% for electroplating wastewater. The reduction in the copper removal efficiency observed with the electroplating waste stream could be related to the competition of other positively charged cations in the waste stream to get adsorbed in the nanoparticle surface. The investigation using the electroplating wastewater proved the versatility of the synthesized nanoparticles to withstand the diversified composition of the industrial wastewater and the removal efficiency obtained (64.8%) was comparable with other methods.

4. Conclusions

Bio-functionalized silver nano particles, synthesized using *H.gracilis,* were successfully employed for the removal of copper from aqueous solution and electroplating waste water. The optimal conditions for the synthesis of AgNPs were enhanced using statistical modeling. The maximum copper removal was found to be 85% at pH 7, temperature 30 °C and nanoparticle dose of 0.9 g/100 ml. The surface functional groups responsible for metal sorption were identified. Monolayer sorption under homogenous conditions was found to happen during the copper removal using silver nanoparticles. Intra-particle diffusion model

represented the experimental data very well. The equilibrium copper uptake capacity obtained in this study was 46.30 mg/g. Reusability of the synthesized nanoparticle for six cycles with the same efficiency proved the economic feasibility of this study.

Author contributions

A.Muthu kumara Pandian, Conceptualization, Methodology, Investigation, Validation, Writing – original draft. B.Gopalakrishnan, Characterization, Writing – review & editing. M.Rajasimman, Methodology, Formal analysis, Writing – review & editing. N.Rajamohan, Resources, Writing – review & editing. C.Karthikeyan, Conceptualization, Writing – review & editing Supervision

Declaration of competing interest

The authors declare that they have no known competing financial interests or personal relationships that could have appeared to influence the work reported in this paper.

References

Aharoni, C., Sparks, D.L., Levinson, S., Ravina, I., 1991. Kinetics of soil chemical reactions: relationships between empirical equations and diffusion models. Soil Sci. Soc. Am. J. 55, 1307–1312. https://doi.org/10.2136/sssaj1991.03615995005500050019x.

Al-Saydeh, S.A., El-Naas, M.H., Zaidi, S.J., 2017. Copper removal from industrial wastewater: a comprehensive review. J. Ind. Eng. Chem. 56, 35–44. https://doi.org/10.1016/j.jiec.2017.07.026.

Ashish, S.S., Aniruddha, M.M., Vikas, V.J., Prakash, D.R., Mansing, A.A., Sanjay, S.K., 2017. Removal of malachite green dye from aqueous solution with adsorption technique using Limonia acidissima (wood apple) shell as low cost adsorbent. Arab. J. Chem. 10, S3229–S3238. https://doi.org/10.1016/j.arabjc.2013.12.019.

Ayla, O., Gorkem, G., Ayla, C., Bahadir, K.K., 2009. Biosorption of copper (II) ions on Enteromorpha prolifera: application of response surface methodology (RSM). Chem. Eng. J. 146, 377–387. https://doi.org/10.1016/j.cej.2008.06.041.

Bai, Y., Rong, F., Wang, H., Zhou, Y., Xie, X., Teng, J., 2011. Removal of copper from aqueous solutions by adsorption on elemental selenium nanoparticles. J. Chem. Eng. Data 56, 2563–2568. https://doi.org/10.1021/je2000777.

Bankar, A., Joshi, B., Kumar, A.R., Zinjarde, S., 2010. Banana peel extract mediated novel route for the synthesis of silver nanoparticles. Colloids Surf. A Physicochem. Eng. Asp. 368, 58–63. https://doi.org/10.1016/j.colsurfa.2010.07.024.

Calderon-Jimenez, B., Johnson, M.E., Montoro Bustos, A.R., Murphy, K.E., Winchester, M.R., Vega Baudrit, J.R., 2017. Silver nanoparticles: Technological advances, societal impacts, and metrological challenges. Front. Chem. 21, 5–6. DOI=10.3389/fchem.2017.00006.

Chauhan, M., Sharma, B., Kumar, R., Chaudhary, G.R., Hassan, A.A., Kumar, S., 2019. Green synthesis of CuO nanomaterials and their proficient use for organic waste removal and antimicrobial application. Environ. Res. 168, 85–95. https://doi.org/10.1016/j.envres.2018.09.024.

Costa, W.D., Bento, A.M.S., Araujo, J.A.S., Menezes, J.M.C., Costa, J.G.M., Cunha, F.A.B., Coutinho, H.D.M., Filho, F.J.P., Teixeira, R.N.P., 2020. Removal of copper (II) ions and lead (II) from aqueous solutions using seeds of Azadirachta indica A. Juss as bioadsorvent. Environ. Res. 183, 109213. https://doi.org/10.1016/j.envres.2020.109213.

Dolgormaa, A., Lv, C.J., Li, Y., Yang, J., Yang, J.X., Chen, P., Wang, H.P., Huang, J., 2018. Adsorption of Cu(II) and Zn(II) ions from aqueous solution by gel/PVA-modified super-paramagnetic iron oxide nanoparticles. Molecules 23 (11), 2982. https://doi.org/10.3390/molecules23112982.

Dolphen, R., Thiravetyan, T., 2011. Adsorption of melanoidins by chitin nanofibers. Chem. Eng. J. 166, 890–895. https://doi.org/10.1016/j.cej.2010.11.063.

Dong, J., Du, Y., Duyu, R., Shang, Y., Zhang, S., Han, R., 2019. Adsorption of copper ion from solution by polyethylenimine modified wheat straw. Bioresour. Technol. Rep. 6, 96–102. https://doi.org/10.1016/j.biteb.2019.02.011.

Duarte-Nass, C., Rebolledo, K., Valenzuela, T., Kopp, M., Jeison, D., Rivas, M., Azocar, L., Torres-Aravena, A., Ciudad, G., 2020. Application of microbe-induced carbonate precipitation for copper removal from copper-enriched waters: challenges to future industrial application. J. Environ. Manag. 256, 109938. https://doi.org/10.1016/j.jenvman.2019.109938.

Emine, Y.K.C., Kadir, K., 2010. Biosorption of Cu^{2+} and Zn^{2+} by raw and autoclaved Rocella phycopsis. J. Environ. Sci. 22 (3), 367–373. https://doi.org/10.1016/S1001-0742(09)60117-0.

Fernandez-Gonzalez, F., Martin-Lara, M.A., Blazquez, G., Tenorio, G., Calero, M., 2020. Hydrolyzed olive cake as novel adsorbent for copper removal from fertilizer industry wastewater. J. Clean. Prod. 268, 121935. https://doi.org/10.1016/j.jclepro.2020.121935.

Grimm, A., Zanzi, R., Bjornbom, E., Cukierman, A.L., 2008. Comparison of different types of biomasses for copper biosorption. Bioresour. Technol. 99, 2559–2565. https://doi.org/10.1016/j.biortech.2007.04.036.

Gulay, B., Yakup, A.M., 2009. Construction a hybrid biosorbent using Scenedesmus quadricauda and Ca-alginate or biosorption of Cu (II), Zn (II) and Ni (II): kinetics and equilibrium studies. Bioresour. Technol. 100, 186–193. https://doi.org/10.1016/j.biortech.2008.05.050.

Gunasundari, E., Senthil Kumar, P., 2017. Adsorption isotherm, kinetics and thermodynamic analysis of Cu(II) ions onto the dried algal biomass (Spirulina platensis). J. Ind. Eng. Chem. 56, 129–144. https://doi.org/10.1016/j.jiec.2017.07.005.

Harsha Vardhan, K., Senthil Kumar, P., Panda, Rames C., 2019. A review on heavy metal pollution, toxicity and remedial measures: Current trends and future perspectives. J. Mol. Liq. 290, 111197. https://doi.org/10.1016/j.molliq.2019.111197.

Ho, Y.S., 2004. Citation review of Lagergen Kinetic rate equation on adsorption reactions. Scientometrics 59, 171–177. https://doi.org/10.1023/B:SCIE.0000013305.99473.cf.

Ho, Y.S., McKay, G., 1999. Pesudo-second order model for sorption processes. Process Biochem. 34, 451–465. https://doi.org/10.1016/S0032-9592(98)00112-5.

Jayakumar, R., Rajasimman, M., Karthikeyan, C., 2015. Sorption and desorption of hexavalent chromium using a novel brown marine algae Sargassum myriocystum. Kor. J. Chem. Eng. 32 (10), 2031–2046. https://doi.org/10.1007/s11814-015-0036-8.

Kadir, A., Joseph, R., Lakowiez, 2005. Rapid deposition of triangular silver nanoplates on planar surfaces: application to metal-enhanced fluorescence. J. Phys. Chem. 109 (B), 6247–6251. https://doi.org/10.1021/jp044235z.

Karimi, H., Mousavi, S., Sadeghian, B., 2012. Silver nanoparticle loaded on activated carbon as efficient adsorbent for removal of methyl orange. Indian J. Sci. Technol. 2346–2353. https://doi.org/10.17485/ijst/2012/v5i3.3.

Liu, F., Zhou, K., Chen, Q., Wang, A., Chen, W., 2019. Application of magnetic ferrite nanoparticles for removal of Cu(II) from copper-ammonia wastewater. J. Alloys Compd. 773, 140–149. https://doi.org/10.1016/j.jallcom.2018.09.240.

Marimuthu, S., Antonisamy, A.J., Malayandi, S., Rajendran, K., Tsai, P.C., Pugazhendhi, A., Ponnusamy, V.K., 2020. Silver nanoparticles in dye effluent treatment: a review on synthesis, treatment methods, mechanisms, photocatalytic degradation, toxic effects and mitigation of toxicity. J. Photochem. Photobiol., B 205, 111823. https://doi.org/10.1016/j.jphotobiol.2020.111823.

Mie, G., 1908. Contributions to the optics of turbid media especially colloidal metal solutions. Ann. Phys. 25, 377–445. https://doi.org/10.1002/andp.19083300302.

Mondal, S., Majumder, S.K., 2019. Honeycomb-like porous activated carbon for efficient copper (II) adsorption synthesized from natural source: kinetic study and equilibrium isotherm analysis. J. Environ. Chem. Eng. 7, 103236. https://doi.org/10.1016/j.jece.2019.103236.

Muthu Kumara Pandian, A., Rajasimman, M., Rajamohan, N., Varjani, Sunita, Karthikeyan, C., 2021. Anaerobic mixed consortium (AMC) mediated enhanced biosynthesis of silver nano particles (AgNPs) and its application for the removal of phenol. J. Hazard Mater. 125717 https://doi.org/10.1016/j.jhazmat.2021.125717.

Onal, Y., 2006. Kinetics of adsorption of dyes from aqueous solutions using apricot. J. Hazard Mater. 137 (B), 1719. https://doi.org/10.1016/j.jhazmat.2006.05.036.

Ozer, A., Akkaya, G., Turabik, M., 2006. Biosorption of acid blue 290 (AB 290) and acid blue 324 (AB 324) dyes on Spirogyra rhizopus. J. Hazard Mater. 135 (1), 355–364. https://doi.org/10.1016/j.jhazmat.2005.11.080.

Pagnanelli, F., Trifoni, M., Beolchini, F., Esposito, A., Toro, L., Veglio, F., 2001. Equilibrium biosorption studies in single and multi-metal systems. Process Biochem. 37, 115–124. https://doi.org/10.1016/S0032-9592(01)00180-7.

Rajamohan, N., Rajasimman, M., 2016. Biosorptive removal of heavy metal onto raw activated sludge-Parametric, equilibrium and kinetic studies. J. Environ. Eng. 142 (9), 1–7. https://doi.org/10.1061/(ASCE)EE.1943-7870.0000961.

Rajasimman, M., Rajamohan, N., Sujatha, S., 2021. Recovery of zinc from electroplating wastewater using green emulsion liquid membrane. Water Supply ws2020294. https://doi.org/10.2166/ws.2020.294.

Rajeshkannan, R., Rajamohan, N., Rajasimman, M., Sivaprakash, B., 2010. Equilibrium and kinetic studies on sorption of malachite green using Hydrilla Verticillata biomass. Int. J. Environ. Res. 4 (4), 817–824. https://doi.org/10.22059/IJER.2010.268.

Rastogi, L., Arunachalam, J., 2013. Green synthesis route for the size controlled synthesis of biocompatible gold nanoparticles using aqueous extract of garlic (Allium sativum). Adv. Mater. Lett. 4 (7), 548–555. https://doi.org/10.5185/amlett.2012.11456.

Ravichandran, V., Xin, T.Z., Gunasagaran, S., Xiang, T.F.W., Yang, E.F.C., Jeyakumar, N., Dhanaraj, S.A., 2011. Biosynthesis of silver nanoparticles using mangosteen leaf extract and evaluation of their antimicrobial activities. J. Saudi Chem. Soc. 15 (2), 113–120. https://doi.org/10.1016/j.jscs.2010.06.004.

Safari, E., Rahemi, N., Kahforoushan, D., Allahyari, S., 2019. Copper adsorptive removal from aqueous solution by orange peel residue carbon nanoparticles synthesized by combustion method using response surface methodology. J. Environ. Chem. Eng. 7, 102847. https://doi.org/10.1016/j.jece.2018.102847.

Sathishkumar, M., Sneha, K., Won, S.W., Cho, C.W., Kim, S., Yun, Y.S., 2009. Cinnamon zeylanicum bark extract and powder mediated green synthesis of nano-crystalline silver particles and its bactericidal activity. Colloids Surf., B 73, 332–338. https://doi.org/10.1016/j.colsurfb.2009.06.005.

Shahrashoub, M., Bakhtiari, S., 2021. The efficiency of activated carbon/magnetite nanoparticles composites in copper removal: industrial waste recovery, green synthesis, characterization, and adsorption-desorption studies. Microporous Mesoporous Mater. 311, 110692. https://doi.org/10.1016/j.micromeso.2020.110692.

Surya, K.M., Jai, P.G., 2001. Removal of Ni and Cu from single and binary metal solutions by free and immobilized Chlorella vulgaris. Eur. J. Protistol. 37, 261–271. https://doi.org/10.1078/0932-4739-00813.

Vanaja, M., Paulkumar, K., Baburaja, M., 2014. Degradation of methylene blue using biologically synthesized silver nanoparticles. Bioinorgan. Chem. Appl. 1, 1–7. https://doi.org/10.1155/2014/742346.

Venkatesh Babu, S., Rajasimman, M., Rajamohan, N., 2017. Biodegradation of textile dyeing industry wastewater using modified anaerobic sequential batch reactor - Start up, parameter optimization and performance analysis. J. Taiwan Inst. Chem. Eng. 72, 171–181. https://doi.org/10.1016/j.jtice.2017.01.027.

Volesky, B., 2003. Sorption and Biosorption. BV-Sorbex Inc., Quebec, Canada.

Weber, W.J., Morris, J.C., 1963. Kinetics of adsorption on carbon from solution. J. Sanit. Eng. Div. ASCE. 89, 31–60.

Yaqoob, A.A., Umar, K., Ibrahim, M.N.M., 2020. Silver nanoparticles: various methods of synthesis, size affecting factors and their potential applications–a review. Appl. Nanosci. 10, 1369–1378. https://doi.org/10.1007/s13204-020-01318-w.

Yi, C.L., Shui, P.C., 2011. The biosorption of heavy metals from aqueous solution by Spirogyra and Cladophora filamentous macroalgae. Bioresour. Technol. 102, 5297–5304. https://doi.org/10.1016/j.biortech.2010.12.103.

Zhang, J., Lin, S., Han, M., Su, Q., Xia, L., Hui, Z., 2020. Adsorption properties of magnetic magnetite nanoparticle for coexistent Cr(VI) and Cu(II) in mixed solution. Water 12, 446. https://doi.org/10.3390/w12020446.